Fourth International Conference on Sustainable Construction Materials and Technologies
http://www.claisse.info/Proceedings.htm

SCMT4

Las Vegas, USA, August 7-11, 2016

Carbonation Reaction Kinetics, CO_2 Sequestration Capacity, and Microstructure of Hydraulic and Non-Hydraulic Cementitious Binders

Warda Ashraf[1], Jan Olek[2], and Vahit Atakan[3]

[1]*Graduate Research Assistant, Lyles School of Civil Engineering, Purdue University, West Lafayette, IN 47907, USA. Email: washraf@purdue.edu*

[2]*Professor, Lyles School of Civil Engineering, Purdue University, West Lafayette, IN 47907, USA. Email: olek@purdue.edu*

[3]*Director, Research and Development, Solidia Technologies, NJ, USA. Email: vahit@solidiatech.com*

ABSTRACT

This paper presents a study on the carbonation curing of hydraulic (i.e., ordinary portland cement, OPC) and non-hydraulic (i.e., calcium silicate based cement, CSC) cementitious materials. The primary components of CSC are low-lime calcium silicates such as rankinite, wollastonite, and pseudo-wollastonite. The major difference between CSC and OPC system is that the CSC system generates strength from the carbonation reaction while strength development of OPC system depends on the hydration reaction. Nonetheless, CSC can be used to prepare concrete with mechanical properties similar to that of OPC. Thermogravimetric analysis (TGA) was used to monitor the rate of carbonation of the paste samples. The CO_2 sequestration capacity of OPC was found to be slightly (~3%) higher than that of the CSC.

INTRODUCTION

The increasing rate of greenhouse gas emission has created a demand for man-made sinks of CO_2 and other greenhouse gases. Accordingly, several recent research works have been focused on the possibility of storing CO_2 in cement-based materials (El-Hassan & Shao 2014; Kashef-Haghighi & Ghoshal 2010; Mo & Panesar 2013; Monkman & Shao 2010; Shao et al. 2006; Siriwardena & Peethamparan 2015). The CO_2 storing capacity of cement-based materials is dependent on their chemical compositions, more specifically on the oxides contents (Huntzinger et al. 2009; Siriwardena & Peethamparan 2015). In this regard, Steinour (Steinour 1959) has proposed a formula (as given in Eq. 1) to calculate the maximum theoretical amount (%) of CO_2 that can be stored in cement based materials considering their oxide contents.

$$CO_2\ (\%, max) = 0.785(CaO - 0.7SO_3) + 1.091\ MgO + 1.420\ Na_2O + 0.935\ K_2O \quad (1)$$

In addition to the CO_2 sequestration capacity, the kinetics of carbonation reaction of cement-based materials is of much interest (Galan et al. 2013; Papadakis et al. 1991). Most of the existing carbonation kinetic models were developed to predict the depth of carbonation in hardened concrete while subjected to accelerated carbonation exposure conditions. In these experimental cases, the diffusion coefficient of CO_2 through the pores of hardened microstructure of concrete plays the dominant role. In order to store a substantial amount of CO_2, usually the cement paste or concrete samples are subjected to carbonation curing in fresh state (usually immediately after mixing (Kashef-Haghighi & Ghoshal 2010; Monkman & Shao 2010)). Kinetics of the chemical reaction between CO_2 and anhydrous cement in the presence of moisture is expected to play the dominant role in such cases. Only a few studies (Galan et al. 2013; Huntzinger et al. 2009) focused on the chemical kinetics of this carbonation reaction of cement-based materials have been performed till now. As such, and considering the recent interest on CO_2 storing in the cementitious materials additional investigation on carbonation kinetics are warranted (Ashraf 2016). Similar to the CO_2 sequestration capacity, the carbonation reaction kinetics can also be expected to depend on the chemical composition of the raw material.

In this paper, we have compared the carbonation behavior of OPC and CSC pastes. The CSC is a newly developed binder system produced by Solidia Technologies (Sahu & DeCristofaro 2013), following the methods described in the US patents (Riman, Gupta, Atakan, & Li 2013; Riman, Nye, Atakan, Vakifahmetoglu, Li, & Tang 2015). This cement is primarily composed of low-lime calcium silicates such as wollastonite, pseudo-wollastonite and rankinite (Sahu & DeCristofaro 2013). These low-lime calcium silicate phases are essentially non-hydraulic but can be reactive in the presence of both water and CO_2 (Bukowski & Berger 1978; Ashraf, Olek & Atakan 2015a; Ashraf & Olek 2016). Thus, the hardening of CSC binder system relies on the carbonation reaction. A compressive strength of 8000 psi to 11600 psi can be achieved from CSC concrete by controlling the degree of carbonation (Jain et al. 2014). Concrete samples prepared using CSC binder were also observed to provide adequate resistance from freeze-thaw, scaling, and deicing salt damages (Jain et al. 2015; Farnam et al. 2016). During the carbonation reaction, the CSC binder forms calcium carbonate and silica gel (also known as calcium-modified silica gel) which are the primary microscopic phases present in this system (Jain et al. 2014). The degree of silicate polymerization and stiffness of the silica gel phase was found to be substantially higher than that of calcium silicate hydrates (C-S-H) (Ashraf, Olek & Tian 2015; Ashraf, Olek & Atakan 2015b; Ashraf & Olek 2016). However, the kinetics of carbonation reaction of this binder system has not been thoroughly investigated yet and hence; it is one of the research objectives of this paper. In addition to the kinetics of carbonation reaction, this paper also determined the CO_2 sequestration capacity of CSC and OPC binders.

EXPERIMENTAL PROCEDURE

Materials

The CSC used in the experiments was supplied by Solidia Technologies. Figure 1 shows the particle size distribution of the CSC cement as obtained using a laser particle size analyzer considering a refractive index of 1.63. The CaO content (by mass) of CSC binder is in the range of 40% to 45% (the complete results of the X-ray fluorescence test are not shown in this paper). In the case of OPC (Type-I) system, the CaO content usually ranges from 60% to 67% (Wikipedia, 2015). Thus, considering the CaO contents and using the Steinour (Steinour 1959) formula, the CO_2 sequestration capacity of OPC binder should be 30% to 60% higher than that of CSC. To prepare the paste samples, first, approximately 20 gm of cement samples were mixed with water. Four different water to cement (w/c) ratios were used, these were: 0.2, 0.3, 0.4 and 0.5. After 2 minutes of hand mixing, the paste samples were spread on plastic plates without any compaction. Samples prepared using this method had an average dimension of 1~2 mm. For the small dimensions (1~2 mm) of the samples used in this work, it was assumed that the carbonation reaction is

uniform throughout the sample. These paste samples were then subjected to carbonation reaction using the following conditions: 10% CO_2 concentration, temperature of 30ºC and 94% RH. To monitor the effect of temperature, a separate batch of paste samples (w/c = 0.4) ratio was exposed to carbonation at 10% CO_2 concentration, temperature of 60ºC and 94% RH. Approximately 2 gm of samples were collected from each batch of the pastes after 0.5, 3, 6, 11, 24, 60, 97 and 145 hours of carbonation curing. Collected paste samples were ground using mortar-pestle and then, examined using TGA to determine the $CaCO_3$ and water contents.

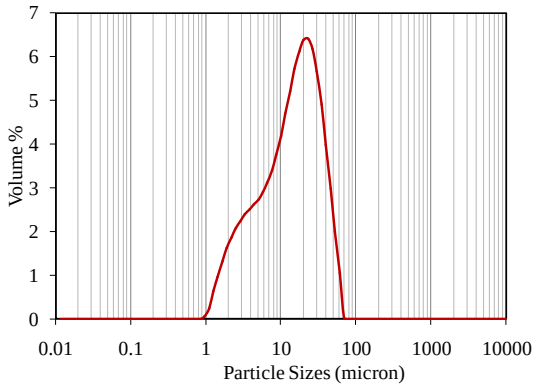

Figure 1. Particle size distribution of CSC cement.

RESULTS AND DISCUSSIONS

Thermogravimetric analysis (TGA) results

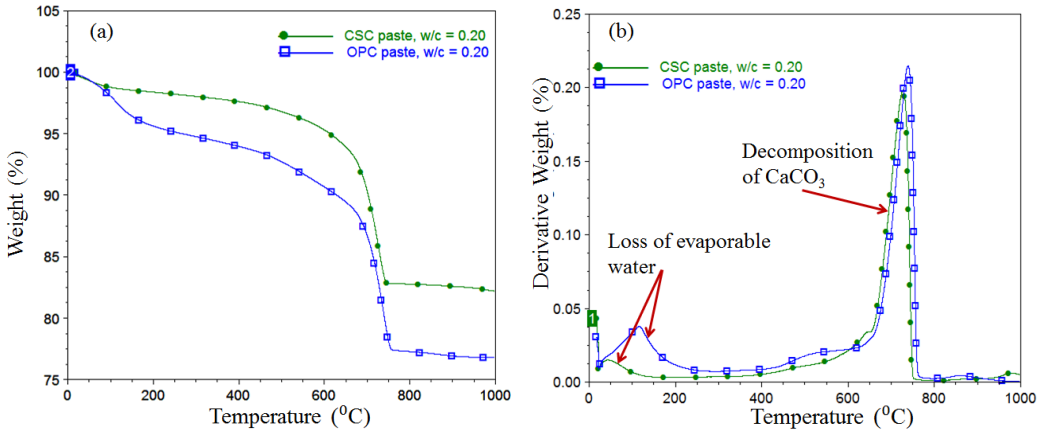

Figure 2. TGA (a) and DTG (b) curves for carbonated CSC and OPC paste samples

Figure 2 shows the TGA (a) and derivative of thermogravimetric (DTG) (b) graphs for carbonated CSC and OPC paste (w/c ratio = 0.20) samples after 145 hours of carbonation. Two major mass losses can be observed in the DTG graph (Figure 2 (b)) for both types of the paste samples. The mass loss below 180ºC is attributed to the loss of evaporable water of the samples. Decomposition of $CaCO_3$ and concurrent release of CO_2 contributes the mass loss in the temperature range of from 450 ºC to 800 ºC. The reaction associated with this process is given by Eq.2

$$CaCO_3\ (s) \rightarrow CO_2\ (g) + CaO\ (s) \qquad (2)$$

It is important to note that none of the carbonated samples contained $Ca(OH)_2$ as indicated by the absence of the characteristic peak in the temperature range of 350 ºC to 450 ºC of the DTG graph. The absence of this peak confirms complete carbonation of the OPC samples. The $Ca(OH)_2$ peak was not expected to be present in the CSC paste as this material is non-hydraulic. Using the mass losses obtained from TGA results and the stoichiometric equation for $CaCO_3$ decomposition (Eq.2), the relative proportion of $CaCO_3$ present in the carbonated samples were determined and analyzed as described in the following sections of this paper.

Carbonation kinetics

To analyze the carbonation kinetics of CSC and OPC paste samples, the degree of carbonation (DOC) was calculated using following equation:

$$Normalized\ degree\ of\ carbonation\ (DOC)\ at\ time\ t$$

$$= \frac{CaCO_3\ content\ (mass, percentage) at\ time\ t}{Maximum\ CaCO_3 content\ (mass, percentage)\ after\ 145\ hours\ of\ carbonation} \times 100\% \quad (3)$$

The highest amount of $CaCO_3$ formed in any batches of the pastes for each type of cement after 145 hours of carbonation reactions was considered to be the maximum $CaCO_3$ content in eq.3. These maximum $CaCO_3$ contents were found to be 45.39% and 39.9% for OPC and CSC paste samples, respectively. The changes in the degree of carbonation with an increase in the exposure time for CSC and OPC pastes are given in

Figure 3 (a) and (b), respectively. Analysis of the data presented in

Figure 3 (a) and (b) indicates that the carbonation reaction of the cement pastes occurs in two different stages. In stage 1 (marked as (1) in

Figure 3 (a) and (b)) the reaction rate is relatively high and expected to be governed by the dissolution rate of the starting cement phases (Daval et al. 2009). In stage-2 (marked as (2) in

Figure 3 (a) and (b)) the reaction rate is slower than that of the stage-1. The slower reaction rate in stage-2 suggests that during this stage the carbonation reaction rate is controlled by the diffusion of ions through the layers of reaction products formed in stage-1. For both types of cements (CSC and OPC), a lower w/c ratio resulted in the maximum reaction rate during stage-1 of the carbonation reaction. However, when analyzed after 145 hours of carbonation, the amounts of $CaCO_3$ formed were found to increase with the increase in the w/c ratio for both types of the binders. The carbonation reaction kinetics of CSC cement paste samples was observed to follow a simple exponential model (Eq.4) equation. Application of such exponential based reaction kinetics models has also been suggested by several researchers (Daval et al. 2009; Galan et al. 2013; Huntzinger et al. 2009).

$$\alpha = \alpha_0 - A.\exp(-B.t) \quad (4)$$

Here, α_0 is the asymptotic value of the model equation for a given set of carbonation scenario and t is the exposure duration in hours. The coefficients A and B are fitting parameters, which depend on the carbonation scenario. Table 1 shows the fitting parameters and corresponding R^2 values for the proposed reaction models. The model predicted values of the degree of carbonation for the CSC binders are shown as the solid lines in

Figure 3 (a). The models based on Eq.4 were also found to provide a good match to the

experimentally measured degree of carbonation of OPC paste samples but only for systems with low w/c ratio (i.e., w/c = 0.2 and 0.3). For OPC paste samples with higher w/c ratio (i.e., w/c = 0.4 and 0.5), the kinetics of carbonation reaction was found to follow a slightly modified exponential model as given in Eq.5. Unlike in the case of OPC pastes with lower w/c values, the degree of carbonations observed for OPC pastes with higher w/c ratio (i.e., w/c = 0.4 and 0.5) showed a slightly upward trend during the entire duration of stage 2 (see

Figure 3 (b)).

$$\alpha = \alpha_0 - A_1.\exp(-B_1.t) - A_2.\exp(-B_2.t) \quad (5)$$

Here, A_1, A_2, B_1, and B_2 are fitting parameters that vary with experimental conditions. The modeled degree of carbonation (solid line) along with the experimentally measured values (marker points) for OPC pastes are given in

Figure 3 (b).

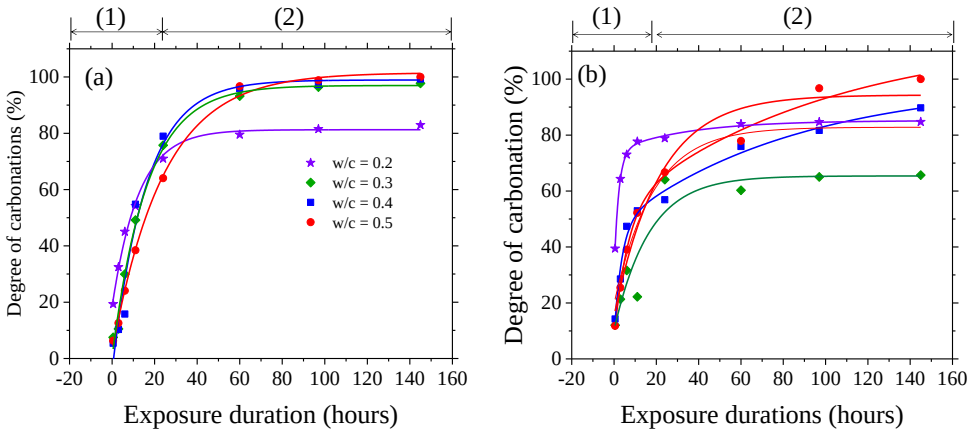

Figure 3. Effects of w/c ratio on the degree of carbonation of (a) CSC paste and (b) OPC paste. Solid lines are the model predicted values and marker points are the experimental values.

Table 1. Fitting parameters for carbonation model.

w/c ratios	CSC paste				OPC paste									
	model Eq.4				model Eq.4				model Eq.5					
	R^2	α_0	A	B	R^2	α_0	A	B	R^2	α_0	A_1	B_1	A_2	B_2
w/c=0.2	0.99	81.26	62.98	0.08	0.97	82.46	49.04	0.29	0.99	115.75	45.65	0.16	62.61	0.01
w/c=0.3	0.99	96.98	96.51	0.06	0.85	65.40	55.15	0.06	0.75	98.87	39.77	0.28	51.42	0.01
w/c=0.4	0.97	98.93	103.48	0.06	0.90	82.82	63.20	0.05	0.98	65.40	27.55	0.06	27.60	0.06
w/c=0.5	0.99	101.52	99.05	0.04	0.92	94.32	79.03	0.04	0.99	85.20	44.10	0.47	10.96	0.03

As can be seen, the kinetic model represented by Eq.5 contains additional exponential term as compared to the model represented by Eq.4. It is important to note that when the OPC specimen is exposed to both, the water and the CO_2, the hydration and carbonation reactions are expected to occur simultaneously. Contradictorily, under the same exposure condition, the CSC pastes will only undergo the carbonation

reaction because of non-hydraulic nature of this binder. Thus, one of the possible explanations for the additional term in Eq.5 (compared to Eq.4) is that it represents the hydration reaction of the OPC pastes that was occurring in parallel with the carbonation reaction.

Evaporable and non-evaporable (chemically bound) water content

The evaporable water content was determined as the percent of the mass loss of the carbonated samples that occurred below 180 ºC using the TGA results. Figure 4 shows the percent of evaporable water with exposure duration for both, CSC and OPC paste systems. Evaporable water can be present either as free water or physically absorbed in the gel phases (C-S-H or silica gel) which formed during the carbonation reaction. From Figure 4 it can be observed that irrespective of the w/c value and the duration of the carbonation cycle the percentage of evaporable water in carbonated OPC paste is always higher than that of the CSC paste samples. This dissimilarity in the amounts of evaporable water might be due to the difference in the phases formed during the carbonation reaction of CSC and OPC pastes.

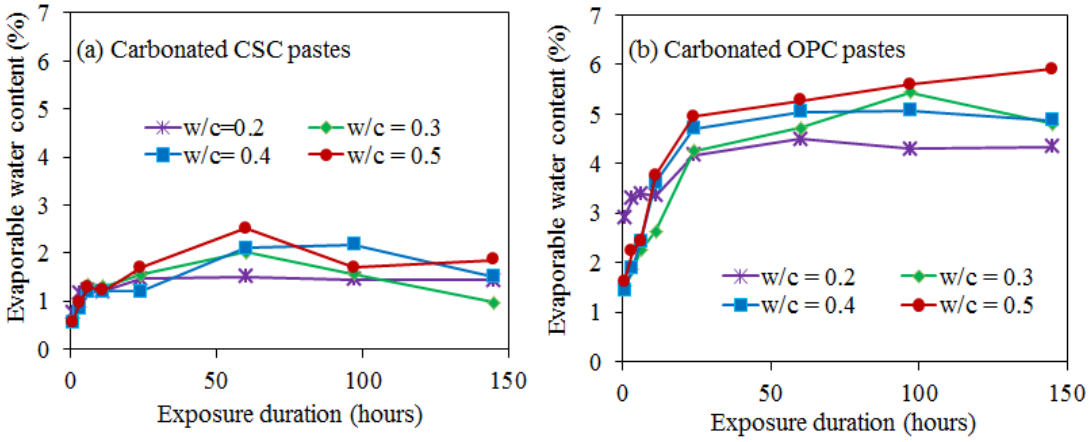

Figure 4. Evaporable water contents of (a) carbonated CSC and (b) carbonated OPC paste systems

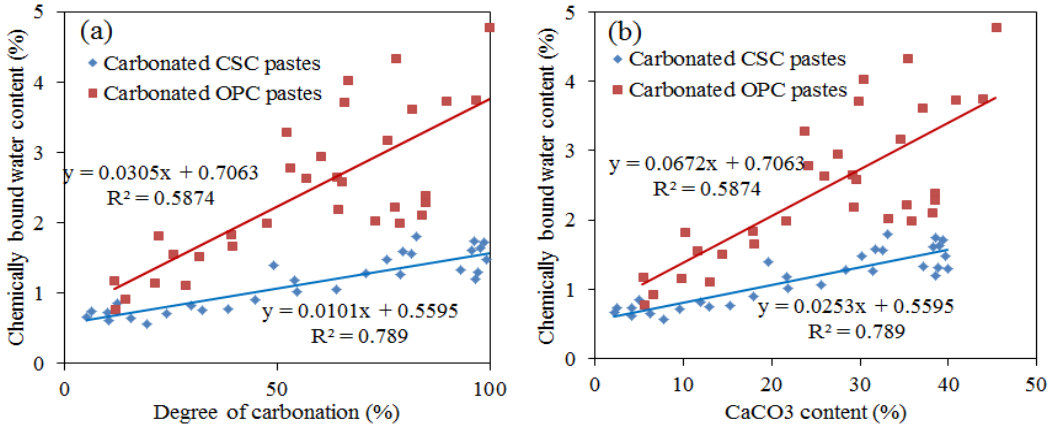

Figure 5: Chemically bound water content in carbonated CSC and OPC paste systems

The total amounts of chemically bound water were determined by subtracting the mass loss due to the decomposition of $CaCO_3$ and evaporable water content from the total mass loss at 1000 ºC. Specifically,

Figure 5 represents the proportion of chemically bound water (also known as structural water of the gel phase) present in the carbonated OPC and CSC systems with (a) different degree of carbonations and (b) $CaCO_3$ contents. In the case of hydrated OPC systems, chemically bound water plays an important role in the reaction kinetics and can be used to directly determine the degree of reaction using Powers' model (Powers & Brownyard 1946). However, in the case of the carbonation reaction, the polymerization and structure of the gel phase are expected to be substantially different than that of the hydrated systems and thus the direct application of Power's model (Powers & Brownyard 1946) is not recommended. From Figure 5 it can be observed that, in case of the carbonated system, a good correlation (considering the R^2 values) exists between the degree of carbonation (or $CaCO_3$ content) and amounts of chemically bound water. This correlation was also observed to be independent of the w/c ratio. Hence, for a well-developed kinetic model of the carbonated cement based system, amounts of chemically bound water can also be used to predict the degree of carbonation and vice-versa. Moreover, from this Figure, it can be observed that for the same degree of carbonation, carbonated OPC system contains a higher proportion of chemically bound water than the non-hydraulic CSC systems. The lower amounts of both, the evaporable and non-evaporable water contents in carbonated CSC paste suggest that the structure of the silica gel phase formed during the carbonation reaction of the CSC system is different than that of the OPC system.

Apparent activation energy of carbonation

Arrhenius equation (Eq.6) is a well-established method to quantify the effect of temperature on reaction rate.

$$k = Zexp\left(-\frac{E_a}{RT}\right) \tag{6}$$

Here, k= carbonation reaction rate; Z = frequency factor (constant); Ea = apparent activation energy kJ/mol; R = universal gas constant (8.315×10^{-3} $kJ.mol^{-1}.K^{-1}$); and T = absolute temperature (K).

Knowing the reaction rate at two different temperatures, the activation energy can be calculated from Eq.7:

$$E_a = R\left[\frac{T_1 T_2}{T_1 - T_2}\ln\left(\frac{k_1}{k_2}\right)\right] \tag{7}$$

The instantaneous carbonation rates of CSC and OPC pastes were determined by taking the derivatives of Eq.4 and Eq.5, respectively. Then using the fitting parameter given in table.1 for w/c = 0.4 and 30ºC the reactions rates for these experimental conditions were calculated. Similarly, a different set of fitting parameters and reaction rates were obtained for w/c = 0.4 and 60ºC. Using these reaction rates at 30ºC and 60ºC, the apparent activation energy of carbonation the cement samples were calculated from Eq.7.

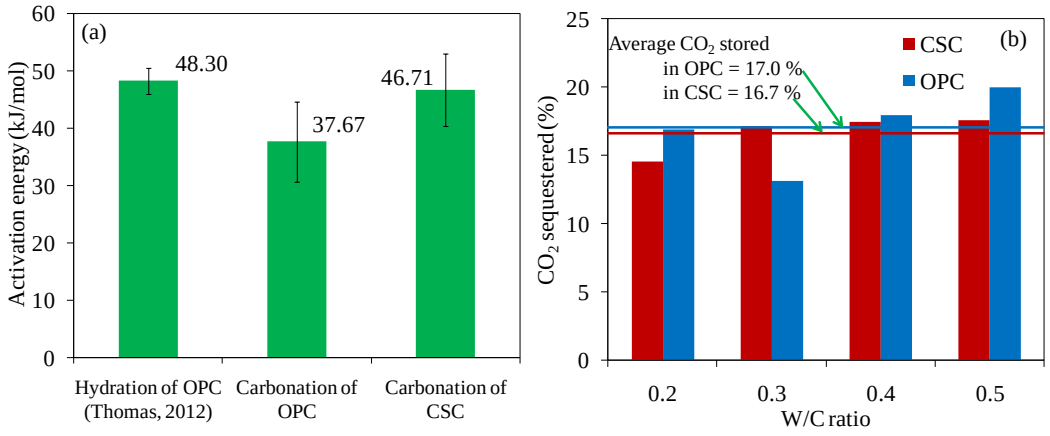

Figure 6. (a) Activation energies for OPC and CSC carbonation, (b) Percent of CO_2 sequestered in OPC and CSC binder systems after 145 hours of exposure in 10% CO_2 concentration

The apparent activation energy for the carbonation of both, OPC and CSC pastes showed slight variation with the degree of carbonation. This is because with increasing degree of carbonation the porosities of pastes were reduced and hence, the unreacted cement particles were lesser accessible to CO_2 and water. Figure 6 (a) shows the average activation energies (average taken for 0 to 85% degree of carbonation) for carbonation of OPC and CSC systems. For comparison purpose, the apparent activation energy for hydration of OPC is also given (Thomas 2012). The apparent carbonation activation energies for both, OPC and CSC systems were lower than those of the hydration of OPC. This indicates, for the given experimental condition, the carbonation rate of these binders were higher than the hydration rate of OPC. OPC had a lower (~ 9kJ/mol) carbonation activation energy than CSC. The higher carbonation activation energy of OPC might have resulted from (i) the simultaneously occurring hydration reaction in OPC pastes and (ii) the differences between the reactants and reaction products of the OPC and CSC systems.

CO_2 sequestration capacity

Figure 6 shows the percent of CO_2 sequestered in OPC and CSC systems after 145 hours of accelerated carbonation in 10% CO_2 environment. For both of the cement paste samples, a slight increase in % of CO_2 stored (< 3%) was observed with increasing w/c ratio. The CaO of OPC cement is approximately 30% to 60% higher than that of the CSC cement. However, the average percent of CO_2 stored in both of these cement types was found to be almost the same (16.7% for CSC and 17.0% for OPC) after 145 hours of carbonation. This contradicts the predicted difference in CO_2 sequestration capacity using the Steinour formula (Steinour 1959) (see experimental procedure section). Apparently, for both types of cements, the carbonation reactions ceased (or were largely hindered) after the formation of the same proportion of carbonation reaction products (i.e., calcium carbonate) which might have covered the available cement surface area required for the continuation of carbonation reaction. Thus, the maximum amounts of the CO_2 stored in both of the cement types were almost same, irrespective of their different CaO content. Similar observations were reported elsewhere (Ashraf & Olek 2016) for the case of pure calcium silicates powders subjected to carbonation reaction under different exposure scenarios.

Microstructure of the carbonated OPC and CSC pastes

The secondary electron (SE)/ SEM images of the carbonated OPC and CSC pastes are given in Figure 7. In the case of carbonated CSC pastes, the gel phase observed to have honeycomb/ lath-like morphology.

Carbonated OPC pastes also contained such lath-like gel phase. However, some needle-like phases of carbonated ettringite were observed to be present in carbonated OPC.

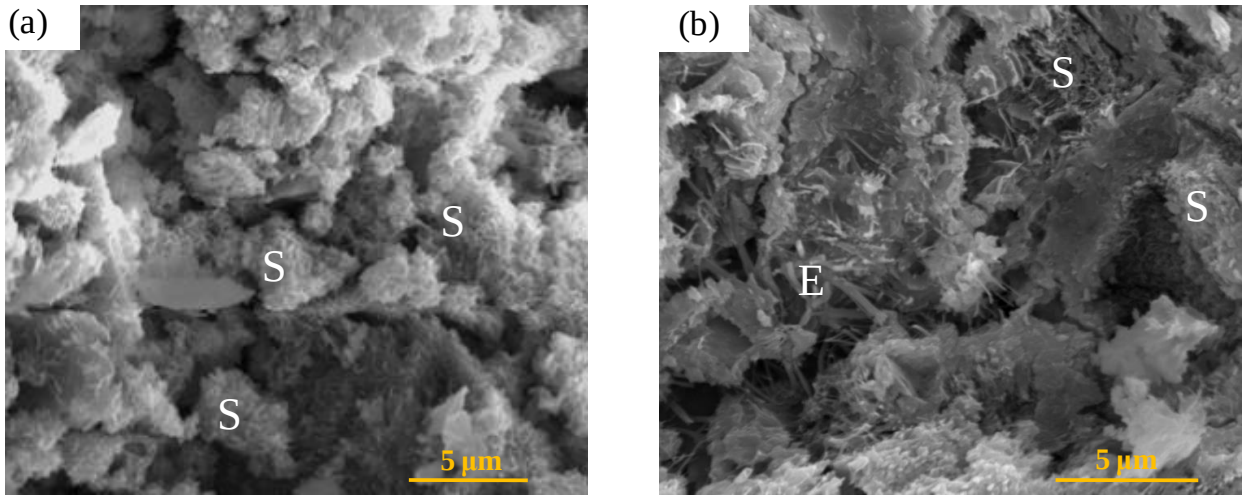

Figure 7. Secondary electron images showing the microstructure of the (a) carbonated CSC paste and (b) carbonated OPC paste (S = silica gel, E = ettringite).

CONCLUSION

The accelerated carbonation kinetics of OPC (hydraulic) and CSC (non-hydraulic) binder systems were investigated in this study. The following conclusions can be formulated based on the analysis of the available data:

1. In general, the carbonation kinetics of both hydraulic and non-hydraulic cementitious binders can be described by simple exponential models. However, while the carbonation kinetics of the CSC binder and low (<0.4) w/c OPC binders can be represented by an asymptotic exponential function, the model for the OPC binder systems with w/c > 0.4 required incorporation of an additional exponential term. This additional term is attributed to the fact that the hydration reaction of the hydraulic binders will be occurring simultaneously with the carbonation reaction.
2. Good correlation was observed between the percent of chemically bound water and the degree of carbonation for both, OPC and CSC systems. Hence, similar to the hydrated system, in case of the carbonation activated binder systems the degree of reaction can be determined from the amount of chemically bound water.
3. Both the evaporable and chemically bound water contents were found to be higher in carbonated OPC system than in the CSC systems. Presence of lower amount of chemically bound water even at the same degree of carbonation suggests that the silica gel phases formed during the carbonation reaction of the CSC binder might have different structure (i.e., silicate polymerization) than that form during the carbonation of OPC.
4. For 0.4 w/c ratio, 10% CO_2 concentration, and 90% RH, the apparent activation energy of the carbonation of CSC and OPC pastes were determined to be 46.71 kJ/mol and 37.67 kJ/mol, respectively.

The average CO_2 sequestration capacity of both of CSC and OPC binders was found to be similar (only about 2% difference) after 145 hours of carbonation using 10% of CO_2. From the results presented in this

study, it was observed that the carbonation reaction kinetics of CSC binder is different than that of OPC. Additional studies need to be performed to understand the effects of RH.

ACKNOWLEDGEMENTS

The partial support of this research by Solidia Technologies is gratefully acknowledged.

REFERENCES

Ashraf, W. (2016). "Carbonation of cement-based materials: challenges and opportunities. Construction and Building Materials." 120, pp.558–570.

Ashraf, W. & Olek, J. (2016). "Carbonation behavior of hydraulic and non-hydraulic calcium silicates: potential of utilizing low-lime calcium silicates in cement based materials." Journal of Materials Science, 51(13), pp.6173–6191.

Ashraf, W., Olek, J. & Atakan, V. (2015a). "A comparative study of the reactivity of calcium silicates during hydration and carbonation reactions." In 14th International Congress on Cement Chemistry. Beijing, China.

Ashraf, W., Olek, J. & Atakan, V. (2015b). "Chemo-mechanical comparison of the carbonation and hydration reaction products of synthetic tricalcium silicate (C_3S)." In 11th Brittle Matrix Composites (BMC). Warsaw, Poland.

Ashraf, W., Olek, J. & Tian, N. (2015). "Nanomechanical characterization of the carbonated wollastonite system." In 5th Nanotechnology in construction (NICOM5). pp. 71–77.

Bukowski, J.M. & Berger, R.L. (1978). "Reactivity and strength development of CO_2 activated non-hydraulic calcium silicates." Cement and Concrete Research, 9, pp.57 – 68.

Daval, D., Martinez, I., Corvisier, J., Findling, N., Goffé, B., and Guyot, F. (2009). "Carbonation of Ca-bearing silicates, the case of wollastonite: Experimental investigations and kinetic modeling." *Chemical Geology*, 265(1-2), 63–78.

El-Hassan, H. & Shao, Y. (2014). "Carbon storage through concrete block carbonation. Journal of Clean Energy Technologies." 2(3), pp.287–291.

Farnam, Y., Villani, C., Washington, T., Spence, M., Jain, J. & Weiss, J. (2016)."Performance of carbonated calcium silicate based cement pastes and mortars exposed to NaCl and $MgCl_2$ deicing salt." *Construction and Building Materials*, 111, 63–71.

Galan, I., Andrade, C., & Castellote, M. (2013). "Natural and accelerated CO_2 binding kinetics in cement paste at different relative humidities." *Cement and Concrete Research*, 49, 21–28.

Huntzinger, D. N., Gierke, J. S., Kawatra, S. K., Eisele, T. C., & Sutter, L. L. (2009). "Carbon dioxide sequestration in cement kiln dust through mineral carbonation." *Environmental Science and Technology*, 43(6), 1986–1992.

Jain, J., Atakan, V., DeCristofaro, N., Jeong, H., & Olek, J. (2015). "Performance of Calcium Silicate-based Carbonated Concretes vs . Hydrated Concretes under Freeze-thaw Environments." *Solidia Technologies, White Paper*. Retrieved from http://solidiatech.com/ on December, 2015

Jain, J., Deo, O., Sahu, S., & DeCristofaro, N. (2014). "Solidia Concrete ™." *Solidia Technologies, White Paper*. Retrieved from http://solidiatech.com/ on December, 2015

Kashef-haghighi, S., & Ghoshal, S. (2010). "CO_2 sequestration in concrete through accelerated

carbonation curing in a flow-through reactor." *Industrial and Engineering Chemistry Researc*h, (49), 1143–1149.

Mo, L., & Panesar, D. K. (2013). "Accelerated carbonation – A potential approach to sequester CO2 in cement paste containing slag and reactive MgO." *Cement and Concrete Composites*, 43, 69–77.

Monkman, S., & Shao, Y. (2010). "Integration of carbon sequestration into curing process of precast concrete." *Canadian Journal of Civil Engineering*, 37(2), 302–310.

Papadakis, V., Vayenas, C., & Fardis, M. (1991). "Fundamental modeling and experimental investigation of concrete carbonation." *ACI Materials Journal*, (88), 363–373.

Powers, T. C., & Brownyard, T. L. (1946). "Studies of the physical properties of hardened portland cement paste." Journal of American Concrete Institute, 18(469), 469–504.

Riman, R. E., Gupta, S., Atakan, V., & Li, Q. (2013). "Bonding element, bonding matrix and composite material having the bonding element, and method of manufacturing thereof." *US patent 20130122267 A1*, Washington, D.C., USA.

Riman, R. E., Nye, T. E., Atakan, V., Vakifahmetoglu, C., Li, Q. & L. Tang (2015). "Synthetic formulations and methods of manufacturing and using thereof." *US patent US 9216926 B2*, Washington, D.C., USA.

Sahu, S., & DeCristofaro, N. (2013). "Solidia Cement ™." *Solidia Technologies, White Paper*. Retrieved from http://solidiatech.com/ on December, 2015.

Shao, Y., Mirza, M. S., & Wu, X. (2006). "CO_2 sequestration using calcium-silicate concrete." *Canadian Journal of Civil Engineering*, 33(6), 776–784.

Siriwardena, D. P., & Peethamparan, S. (2015). "Quantification of CO_2 sequestration capacity and carbonation rate of alkaline industrial byproducts." *Construction and Building Materials*, 91, 216–224.

Steinour, H. H. (1959). "Some effects of carbon dioxide on mortars and concrete-discussion." *Journal of American Concrete Institute*, 50(2), 905–907.

Thomas, J.J., 2012. The instantaneous apparent activation energy of cement hydration measured using a novel calorimetry-based method. Journal of the American Ceramic Society, 95(10), pp.3291–3296.